Comparison of the Corrosion Resistance of Commercial coated steel and hot-dip Zn Coatings under Changing Environmental Conditions

Mateusz Luba, Tomasz Mikolajczyk, Boguslaw Pierozynski[*]

Department of Chemistry, Faculty of Environmental Protection and Agriculture
University of Warmia and Mazury in Olsztyn, Plac Lodzki 4, 10-727 Olsztyn, Poland
[*]E-mail: bogpierozynski@yahoo.ca or boguslaw.pierozynski@uwm.edu.pl

This work reports the results of the corrosion behaviour for materials typically applied for the fabrication of mounting assemblies of photovoltaic (PV) power plants. Here, the corrosion characteristics of commercially available hot-dip Zn-coated steel sheets was compared with that of Magnelis® type steel coating. Electrochemical experiments involved comparative assessment of their corrosion properties by utilizing linear polarization and impedance spectroscopy techniques, under the variable concentration of Na_2SO_4 supporting solution, pH and dissolved oxygen content conditions. Surface and cross-sectional morphology, and elemental composition evaluations of metal-coated electrodes were performed by using SEM and EDX spectroscopy techniques.

1. INTRODUCTION

Increasing global importance of alternative, renewable energy sources is a result of general degradation of the environment during extraction of traditional fossil fuels, gradual depletion of their resources and continuous production of harmful by-products upon combustion process(es) [1,2]. Today, photovoltaic (PV) systems make probably the most widely employed solution for the generation of electrical energy, based on renewable energy sources. In particular, ground-mounted photovoltaic solar assemblies are favoured over conventional rooftop PV systems, as they could be constructed on a larger scale with extended flexibility to adjust their orientation and laying angles [3-6].

Typically, mounting elements of solar PV modules are made of steel, which is widely used by many industries because of its technologically important properties, such as high elongation, strength

and plasticity [7]. Nevertheless, it is always important to ensure proper anti-corrosion protection to the steel-based material under environmental conditions, which otherwise could cause its gradual deterioration and finally complete destruction. High humidity and salinity, a wide range of pH and temperature are conditions, which significantly intensify the rate of the corrosion process [8-11]. This phenomenon is based on a chemical or usually electrochemical interaction between the metallic structure and its surrounding conditions. In addition, electrochemical corrosion process could be significantly intensified by connecting two different metals (or alloys) in a galvanic series, where metal or alloy which is more negative in the galvanic series makes an anode and becomes dissolved in accordance with Faraday's law [12-15].

One of the most effective methods of anti-corrosion protection of steel structures is the employment of different types of metallic coatings. Specifically, various types of zinc coating are utilized to protect steel material against harmful corrosion environment(s) [16-19]. Magnelis®, an innovative protective coating is considered by its manufacturer - ArcelorMittal Company to be significantly more corrosion resistant than typical hot-dip or galvanic type Zn coatings. Magnelis® is prepared through modification of Zn-based metallic coating with 3.5% Al and 3% Mg elements [20].

In this work, we have examined the corrosion behaviour (at its initial stage), comparatively, for commercially made, fresh hot-dip Zn-coated steel sheets and Magnelis®-coated carbon steel materials, exposed to two concentrations of Na_2SO_4 solution, under variable pH and dissolved oxygen electrolyte conditions.

2. EXPERIMENTAL

2.1. Materials

Here, the electrochemical corrosion characteristics were conducted for the following sample materials:

-        Hot-dip Zn-coated steel sample: $50 \times 50 \times 3.15$ mm (*ca.* 80-90 µm Zn thickness);
-        Magnelis®-coated steel sample: $50 \times 50 \times 3.02$ mm (Arcelor-Mittal; *ca.* 25-30 µm thick coating).

Before performing the experiments, all sample materials were initially degreased with ethanol and then were dried in a desiccator for several hours. Electrical connections to electrodes were prepared by means of threaded steel wires, covered with shrinkable polyethylene tubes. All corners of working electrodes were properly taped with epoxy resin, strongly resistant to both acidic, as well as alkaline conditions. In addition, AISI 304 SS (304/0H18N9): $30 \times 30 \times 5.01$ mm stainless steel and SCE: saturated calomel electrode were used as counter and reference electrodes, respectively. An experimental distance between the working and counter electrodes was about 30 mm.

2.2. Solutions

Both 0.1 and 0.5 M electrolyte concentrations of Na_2SO_4 salt (decahydrate pure p.a., Chempur) were made up from ultra-pure water, produced by means of Direct-Q3 UV water purification system

from Millipore. The corrosion properties of selected metal-coated samples were tested at room temperature for the following values of pH: 3, 5, 7, 9 and 11, under two dissolved oxygen concentrations (self- vs. imposed aeration - here referred to as Ox) in the electrolyte. The solutions were oxygenated by means of an aeration pump (Jeneca AP-8803 model). The pH of the electrolytes was adjusted through the addition of aqueous, 0.1 M HCl and NaOH solutions (Polish Chemicals Compounds, p.a. chemicals).

2.3. Experimental methodology

A typical, three-electrode glass-made electrochemical cell and Solartron 12.608 W Full Electrochemical System, consisting of 1260 frequency response analyzer (FRA) and 1287 electrochemical interface (EI), were employed to carry-out all electrochemical corrosion experiments. The above involved periodic recording of corrosion potentials (E_{cor}) vs. SCE for all examined electrodes. In addition, all tested metal-coated samples were subjected to instrumental evaluation of their corrosion current (I_{cor}) and polarization resistance (R_p) parameters (the latter, through the so-called linear *polarization experiments*, performed at ±10 mV around an open circuit/corrosion potential: *ocp*, at a scan-rate of 0.10 mVs^{-1}). On the other hand, for a.c. impedance measurements (conducted at the corresponding *ocp* values), the generator provided an output signal of 5mV in amplitude and the frequency range was swept between 100 kHz and 50 mHz. The instruments were controlled by ZPlot 2.9 or Corrware 2.9 software for Windows (Scribner Associates, Inc.). The conductivity of the solutions, oxygen content and pH evaluations were carried-out by means of HI 9835, HI 9146, and HI 2002-01 meters from Hanna Instruments, respectively.

Moreover, SEM/EDX spectroscopic characterization of the selected, fresh metal-coated samples was conducted by using Merlin FE-SEM microscope (Zeiss), equipped with Bruker XFlash 5010 (with 125 eV resolution) EDX supplement unit.

3. RESULTS AND DISCUSSION

3.1 Spectroscopic examination of fresh metal-coated composite samples

Fig. 1 and Table 1 below present the results of surface spectroscopy (SEM/EDX) examinations of fresh Magnelis®-coated steel sheet (Sample A) and hot-dip Zn-coated steel sheet (Sample B) electrodes. It could be seen in Table 1 that the surface of Magnelis®-coated steel sample is primarily composed of Zn (46.77%), Al (5.84%), Mg (0.91%), C (12.31%) and oxygen (24.95%) elements, which understandably deviates from the bulk Magnelis® composition given in Ref. 20 above. The analogous observation could be made for hot-dip Zn-coatings of Sample B, which (compared to that of Magnelis® coating) is characterized by a considerably increased level of zinc. The above could be supported through the EDX elemental mapping analyses shown in Figs. 1(c) and 1 (d) below.

Table 1. Surface EDX elemental analysis for fresh Magnelis®-coated (Sample A) and hot-dip Zn (Sample B) electrodes.

Element	Norm. C [wt.%]	
	Surface Sample A	Surface Sample B
Carbon	13.39 ± 1.87	13.92 ± 2.04
Oxygen	27.15 ± 3.03	22.23 ± 2.63
Magnesium	0.99 ± 0.08	-
Aluminium	6.36 ± 0.30	-
Sulfur	0.21 ± 0.03	0.26 ± 0.04
Chromium	0.21 ± 0.04	0.46 ± 0.04
Zinc	50.89 ± 1.59	62.64 ± 1.89
Silicon	0.49 ± 0.05	0.13 ± 0.03
Phosphorus	0.19 ± 0.03	-
Calcium	0.07 ± 0.03	-
Chlorine	0.05 ± 0.03	-
Potassium	-	0.11 ± 0.03
Iron	-	0.27 ± 0.04
Total:	100.00	100.00

(a)   **(b)**

(c)   **(d)**
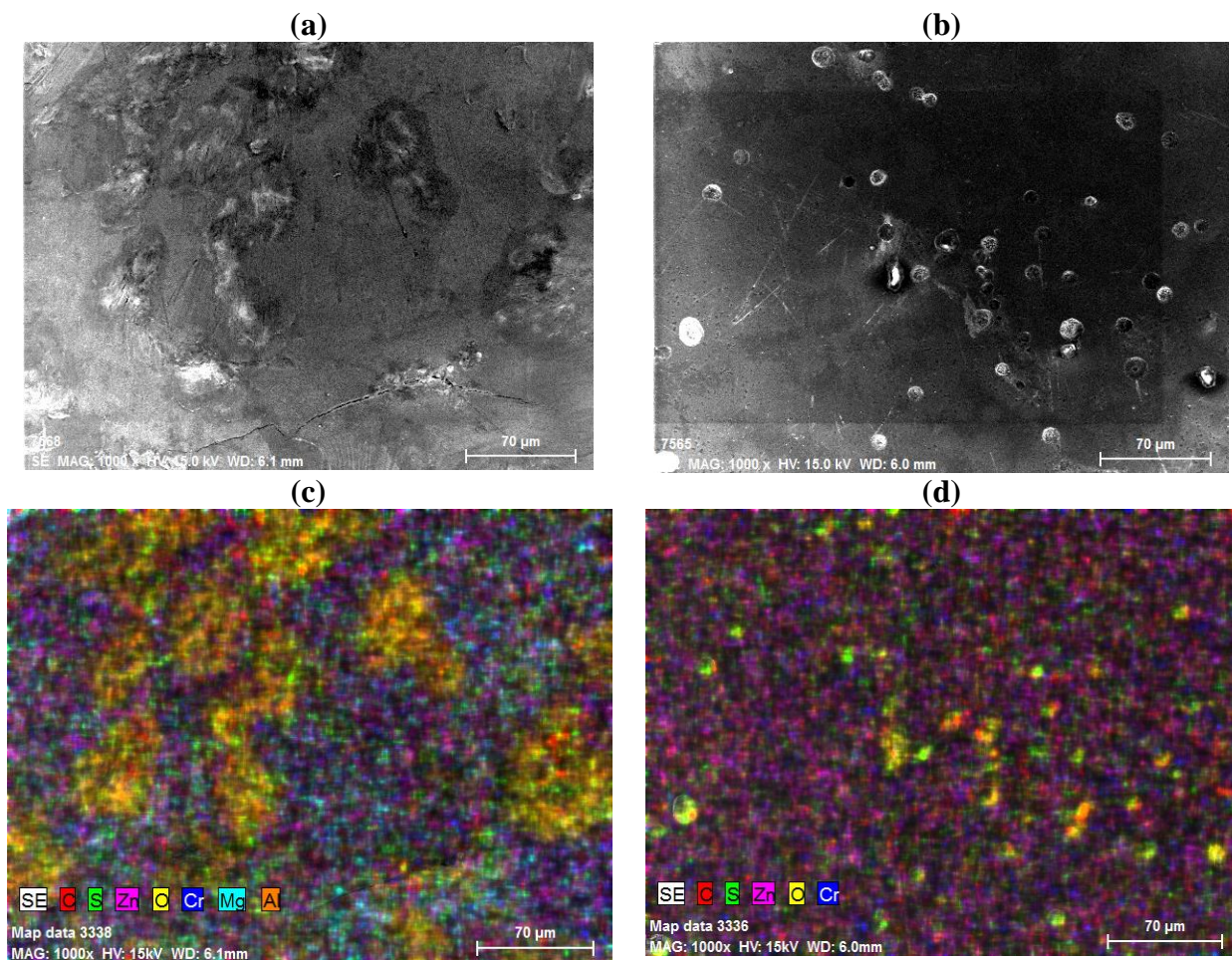
Figure 1. (a) SEM micrograph picture of fresh Magnelis®-coated steel surface, taken at 1000× magnification; (b) SEM micrograph picture of fresh hot-dip Zn-coated carbon steel surface, taken at 1000× magnification; (c) As in (a) above, but EDX mapping, taken at 1000× magnification; (d) As in (b) above, but EDX mapping, taken at 1000× magnification.

3.2 Characteristics of electrochemical corrosion behaviour of steel sheet samples covered with metallic coatings.

At first, the electrochemical corrosion performance of metal-coated samples exposed to Na_2SO_4 environment was studied by means of the linear polarization method. This analysis allowed for the determination of the following parameters: the corrosion current-density (j_{cor}) and polarization resistance (R_p), presented in Table 2.

Table 2. Comparatively calculated average values of corrosion parameters for freshly-exposed hot-dip Zn-coated and Magnelis®-coated steel electrodes, in contact with 0.1 and 0.5 M Na_2SO_4 solutions, obtained through linear polarization measurements.

Conc./M	Materials	E_{cor}/mV	j_{cor}/µA cm^{-2}
0.1 M	Magnelis® (pH 3)	-1067	1.12
	Magnelis® (pH 5)	-1082	0.14
	Magnelis® (pH 7)	-1085	0.16
	Magnelis® (pH 9)	-1084	0.13
	Magnelis® (pH 11)	-1067	0.03
	Hot-dip Zn (pH 3)	-1028	0.90
	Hot-dip Zn (pH 5)	-1088	0.70
	Hot-dip Zn (pH 7)	-1091	0.67
	Hot-dip Zn (pH 9)	-1098	0.41
	Hot-dip Zn (pH 11)	-1067	0.45
0.1 M	Ox Magnelis® (pH 3)	-1074	1.09
	Ox Magnelis® (pH 5)	-1054	0.22
	Ox Magnelis® (pH 7)	-1060	0.29
	Ox Magnelis® (pH 9)	-1078	0.15
	Ox Magnelis® (pH 11)	-1204	0.05
	Ox Hot-dip Zn (pH 3)	-1072	0.94
	Ox Hot-dip Zn (pH 5)	-1059	0.70
	Ox Hot-dip Zn (pH 7)	-1046	0.97
	Ox Hot-dip Zn (pH 9)	-1058	0.99
	Ox Hot-dip Zn (pH 11)	-1046	0.69
0.5 M	Magnelis® (pH 3)	-1075	1.90
	Magnelis® (pH 5)	-1065	0.28
	Magnelis® (pH 7)	-1072	0.30
	Magnelis® (pH 9)	-1082	0.28
	Magnelis® (pH 11)	-1246	0.60
	Hot-dip Zn (pH 3)	-1082	1.88
	Hot-dip Zn (pH 5)	-1089	0.58
	Hot-dip Zn (pH 7)	-1094	0.59
	Hot-dip Zn (pH 9)	-1094	0.47
	Hot-dip Zn (pH 11)	-1098	0.38
0.5 M	OxMagnelis® (pH 3)	-1075	2.97
	OxMagnelis® (pH 5)	-1092	0.38
	OxMagnelis® (pH 7)	-1090	0.62
	OxMagnelis® (pH 9)	-1089	0.40
	OxMagnelis® (pH 11)	-1091	0.09
	Ox Hot-dip Zn (pH 3)	-1052	2.29
	Ox Hot-dip Zn (pH 5)	-1069	0.81
	Ox Hot-dip Zn (pH 7)	-1086	0.88
	Ox Hot-dip Zn (pH 9)	-1070	0.91
	Ox Hot-dip Zn (pH 11)	-1068	0.71

The R_p parameter was calculated as the inverse of the slope of I (current) vs. E (potential), based on micropolarization (±10 mV vs. *ocp*) measurements. The corrosion current (I_{cor}) was then derived from the well-known Stern-Geary relationship (Equation 1). Finally, the corrosion current-

density is calculated based on the geometrical surface area of the electrodes [21].

$$I_{cor} = \frac{b_a b_c}{2.303 R_p (b_a + b_c)} \qquad (1)$$

For the fixed values of Tafel slopes (b_a and b_c) at 120 mV dec^{-1}, Equation 1 takes a simplified form of Equation 2:

$$I_{cor} = 0.026 \times R_p^{-1} \qquad (2)$$

Thus, for practically all examined pH values, Na_2SO_4 concentrations and under both solution aeration conditions(*ca.* 3.5 vs. 6.5 ppm of dissolved oxygen for self-aerated and O_2-saturated solution, respectively), Magnelis® coating was characterized by radically lower corrosion current-densities and thus increased values of the R_p parameter, in relation to the hot-dip Zn coating material (Table 2 and Fig. 2). Hence, as an example, in self-aerated 0.1 M Na_2SO_4 solution (over the pH range 3-11), the j_{cor} parameter changed from 1.12 to 0.03 and 0.90 to 0.45 µA cm^{-2} for the Magnelis® and the hot-dip Zn samples, correspondingly. Interestingly, examined Magnelis® coating exhibited somewhat inferior corrosion behaviour to that of Zn-coated samples in solution with a higher concentration of H^+ ions (pH 3), whereas its corrosion resistance was especially facilitated under "highly" alkaline conditions (pH 11). Furthermore, as expected, increased Na_2SO_4 and dissolved oxygen concentrations, resulted in considerably higher recorded corrosion current-densities for both examined metal-coated materials. On the contrary, the corrosion potential for all changing parameters (with several exceptions) exhibited fluctuation around 1030-1100 mV vs. SCE.
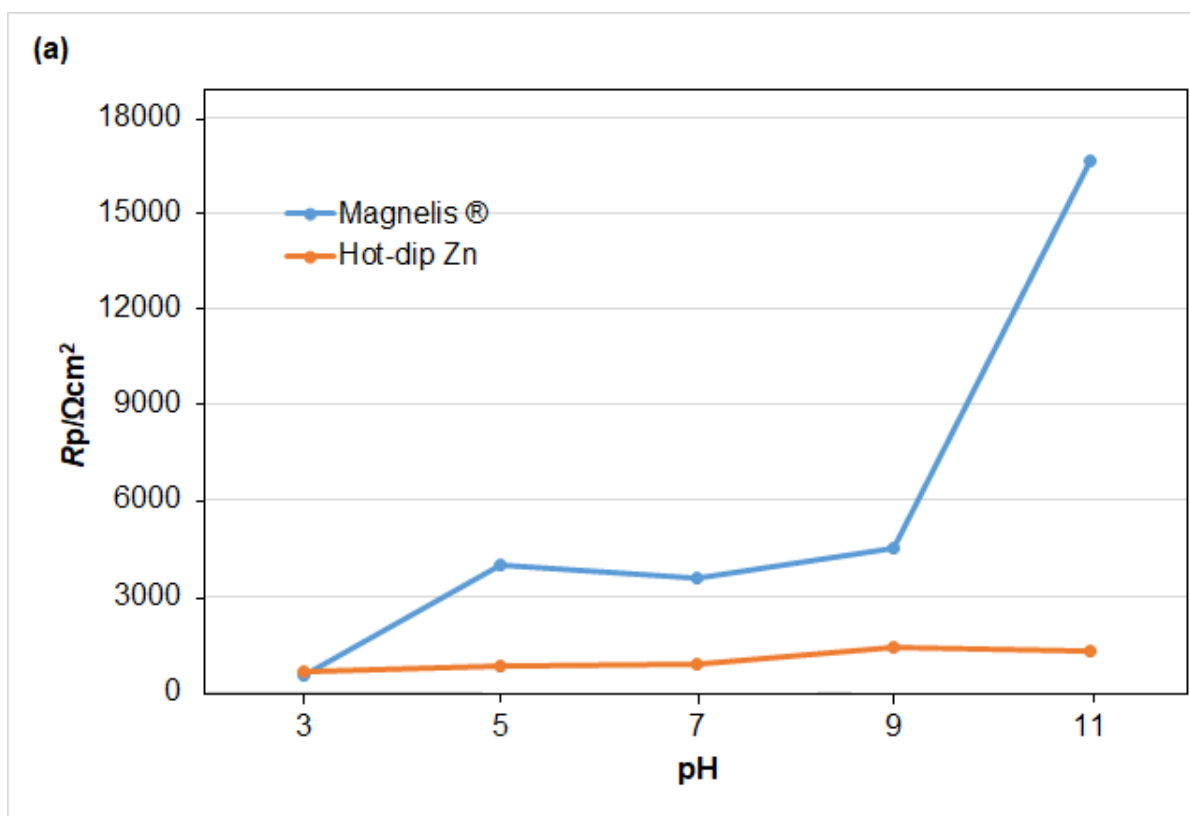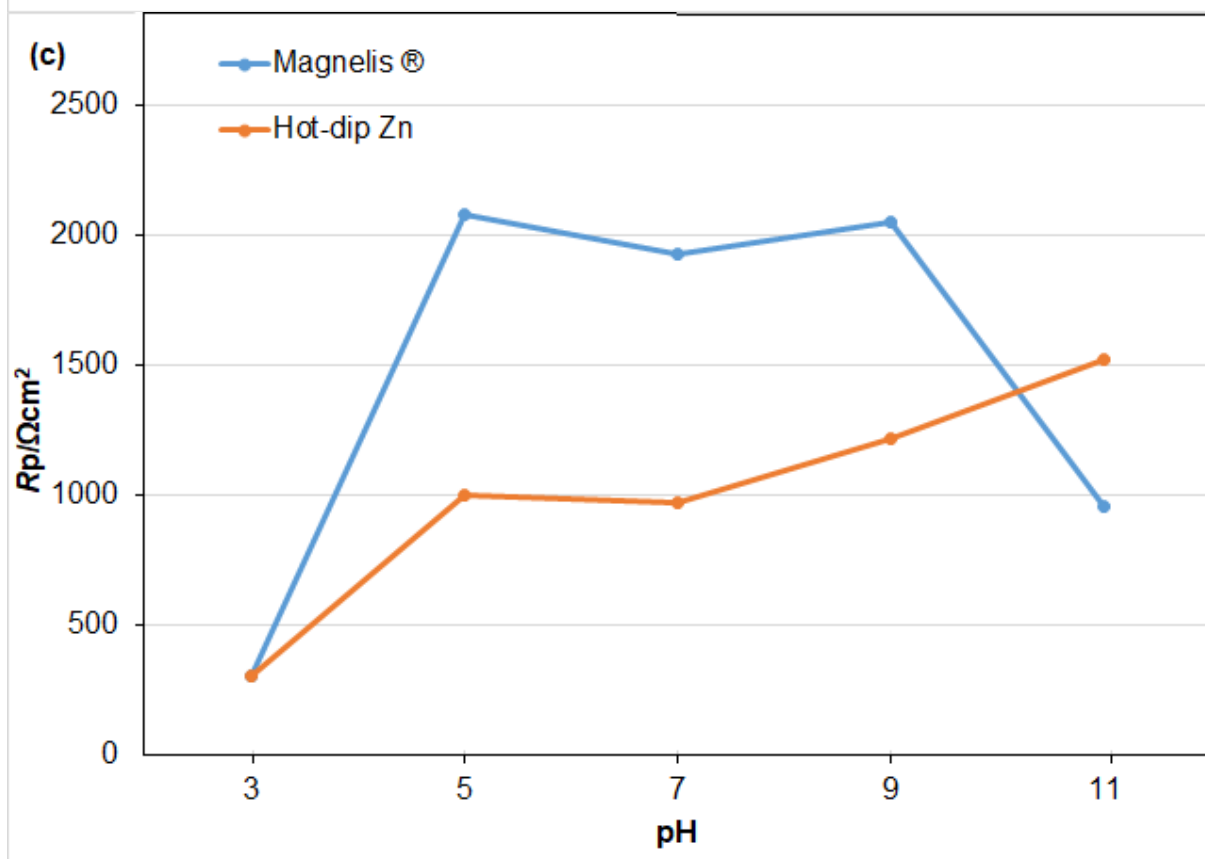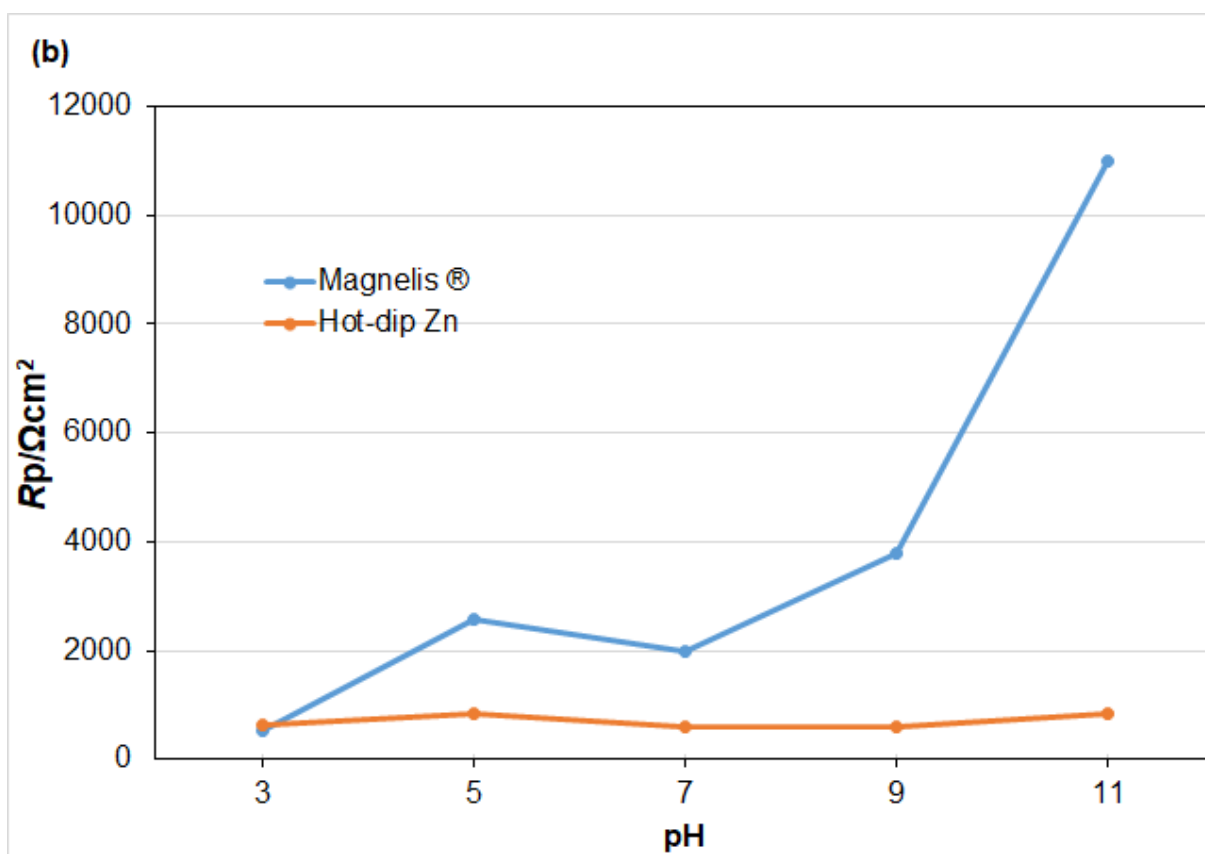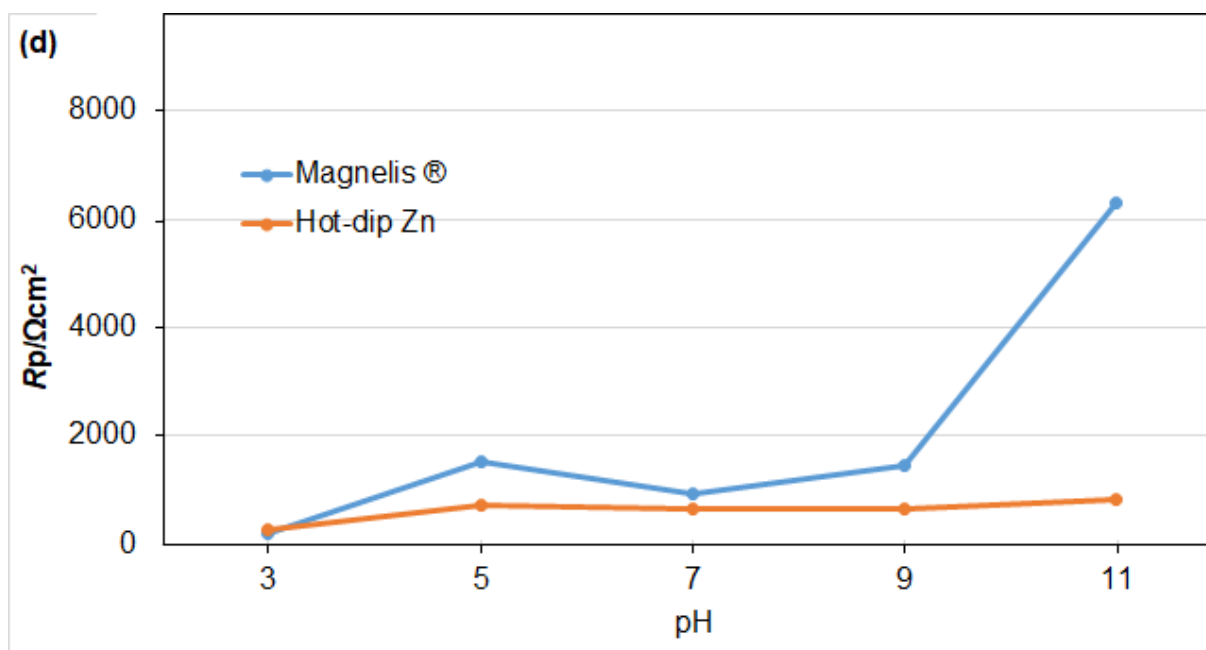
Figure 2. Changes of polarization resistance parameter (R_p) in function of pH for: (a) Self-aerated 0.1 M Na_2SO_4 solution; (b) O_2-saturated 0.1 M Na_2SO_4 solution; (c) As in (a) above, but 0.5 M Na_2SO_4 solution; d) As in (b) above, but 0.5 M Na_2SO_4 solution.

Intensified corrosion rates for the O_2-saturated solutions resulted from the fact that under increased O_2 concentration, cathodic oxygen depolarization reaction (see later Equation 3) became appreciably facilitated, thus also accelerating an anodic, metal surface dissolution phenomenon. On the other hand, a similar experimental trend could also be observed for the related R_p parameter in Fig. 2, where generally (and specifically under alkaline conditions) Magnelis® coating demonstrated considerably larger values of the polarization resistance parameter than those derived for the Zn-coated steel samples.

On the other hand, the impedance characteristics of Zn(Magnelis®)-coated steel electrodes in 0.1 M Na_2SO_4 (at pH 7) were presented in Figs. 3(a) and 3(b), and Table 3. Fig. 3(c) illustrates an equivalent circuit employed for fitting the recorded impedance data, consisting of two constant phase element - CPE-R components, used in order to account for the so-called capacitance dispersion effect [27-29]. Hence, the Nyquist impedance plots [Figs. 3(a) and 3(b)] for Zn/Magnelis®-coated steel electrodes exhibited two somewhat "depressed" semicircles, where a faster process is related to the reaction of charge-transfer resistance (R_{ct}) and interfacial double-layer capacitance (C_{dl}), whereas a slower one is associated with the resistance (R_{coat}) and capacitance (C_{coat}) of the corrosion products accumulated on the electrode surface [22-26], as the corrosion process continues. Most importantly, it could be observed in these Figures that the Magnelis®-coated sample is characterized by radically increased values of the R_{ct} parameter (under both aeration conditions), as compared to that of the Zn-coated sample (6412 vs. 2798 Ω cm^2 for self-aerated solution and 4319 vs. 1300 Ω cm^2 for oxygen-saturated electrolyte, correspondingly, see Table 3 for details). Furthermore, the range of the derived R_{coat} parameter was generally similar for both metal-coated materials and oxygen contents.

In addition, it can also be observed in Table 3 that both C_{dl} and C_{coat} capacitance parameters for

the Zn-coated electrode exhibited radical increase between the two initial experiments, carried-out under the self-aeration and in the O_2-saturation mode (C_{dl}: 8.6-68.1 μF cm^{-2} s$^{\varphi 1-1}$ and C_{coat}: 29.5-93.1 μF cm^{-2} s$^{\varphi 2-1}$), remaining practically unchanged for the Magnelis®-coated sample(total experimental time accounts for about 25 hours). The latter is most likely the result of high sensitivity to the corrosion process, demonstrated by the Zn-coating, thus resulting in an almost immediate change of its surface porosity and structure (contrast to the behaviour at the Magnelis®-based material). Finally, the registered values of dimensionless φ_1 and φ_2 parameters, associated with the the CPE elements, fluctuated around 0.48–0.95.

For both examined metal-coated products, the corrosion phenomenon is primarily initiated with the oxidation of Zn to form Zn^{2+} cations is corrosion environment/solution. This anodic reaction in neutral or alkaline environments is balanced by the process of oxygen depolarization reaction (Equation 3):

$$O_2 + 2H_2O + 4e^- \rightarrow 4OH^- \tag{3}$$

The main corrosion product for Zn coating includes the formation of zinc hydroxide, which is then converted into ZnO, according to Equation 4 [23-25, 30]:

$$Zn^{2+} + 2OH^- \rightarrow Zn(OH)_{2(s)} \rightarrow ZnO_{(s)} + H_2O \tag{4}$$
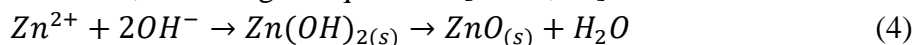
However, compared to typical hot-dip Zn coating, Magnelis® is modified with 3% Mg and 3.5% Al elements. The above leads to the formation of other hydroxide compounds (Equations 5 and 6) [23, 31-34]:

$$Mg^{2+} + 2OH^- \rightarrow Mg(OH)_{2(s)} \tag{5}$$

$$4Al + 3O_2 + 6H_2O \rightarrow 4Al(OH)_{3(s)} \tag{6}$$
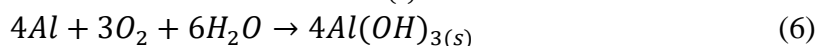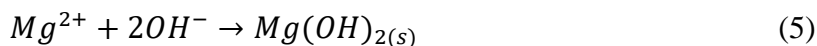
It is commonly known that the addition of Mg and Al compounds to replace Zn is responsible for superior anticorrosive properties of Magnelis® material, in contrast to that displayed solely by the zinc coating [31-32, 35-37]. It is a result of the surface formation of complex, mixed (Mg/Al) hydroxy carbonate precipitates, which form an additional, thin protective coating on the surface of the base material. Moreover, magnesium ions, which precipitate on the surface during the corrosion process, create various products ($Mg(OH)_2$, $MgCO_3$, and $Mg_5(CO3)_4(OH)_2$). These products could locally elevate pH to reach the value of 10-11, which simultaneously impedes the dissolution process of zinc [33].

The current work is a continuation of previously published corrosion articles from this laboratory, on the hot-dip Zn-coated steel and Magnelis®-coated steel materials. In these works [21, 38], the sample materials were subjected to continuous, long-term exposure in 3 wt.% NaCl solution along with a regular assessment of their corrosion parameters by means of the linear and Tafel polarization plots, and ac. impedance spectroscopy techniques. Similarly, results obtained in current work showed improved corrosion properties of Magnelis®-coated material, compared to the traditional Zn-coated steel sample (significantly higher values of R_p and lower values of j_{cor}) [21, 38].

Table 3. The corrosion parameters obtained for Magnelis®-coated and hot-dip Zn-coated steel sheet electrodes, immersed in a neutral solution of 0.1 M Na_2SO_4, derived from a.c. impedance spectroscopy measurements.

R_{ct}/Ω cm^2	R_{coat}/Ω cm^2	$C_{dl}/\mu F$ cm^{-2} s$^{\varphi1-1}$	$C_{coat}/\mu F$ cm^{-2} s$^{\varphi2-1}$
Self-aerated electrolyte			
Hot-dip Zn-coated steel sample			
2798 ±555	10323 ± 567	8.6 ± 0.9	29.5 ± 4.0
Magnelis®-coated steel sample			
6412 ±644	12708 ± 246	20.2 ± 1.3	45.3 ± 1.1
O$_2$-saturated electrolyte			
Hot-dip Zn-coated steel sample			
1300 ±155	9504 ± 324	68.1 ± 6.5	93.1 ± 1.7
Magnelis®-coated steel sample			
4319 ±206	10152 ± 261	21.1 ± 0.9	47.8 ± 1.6
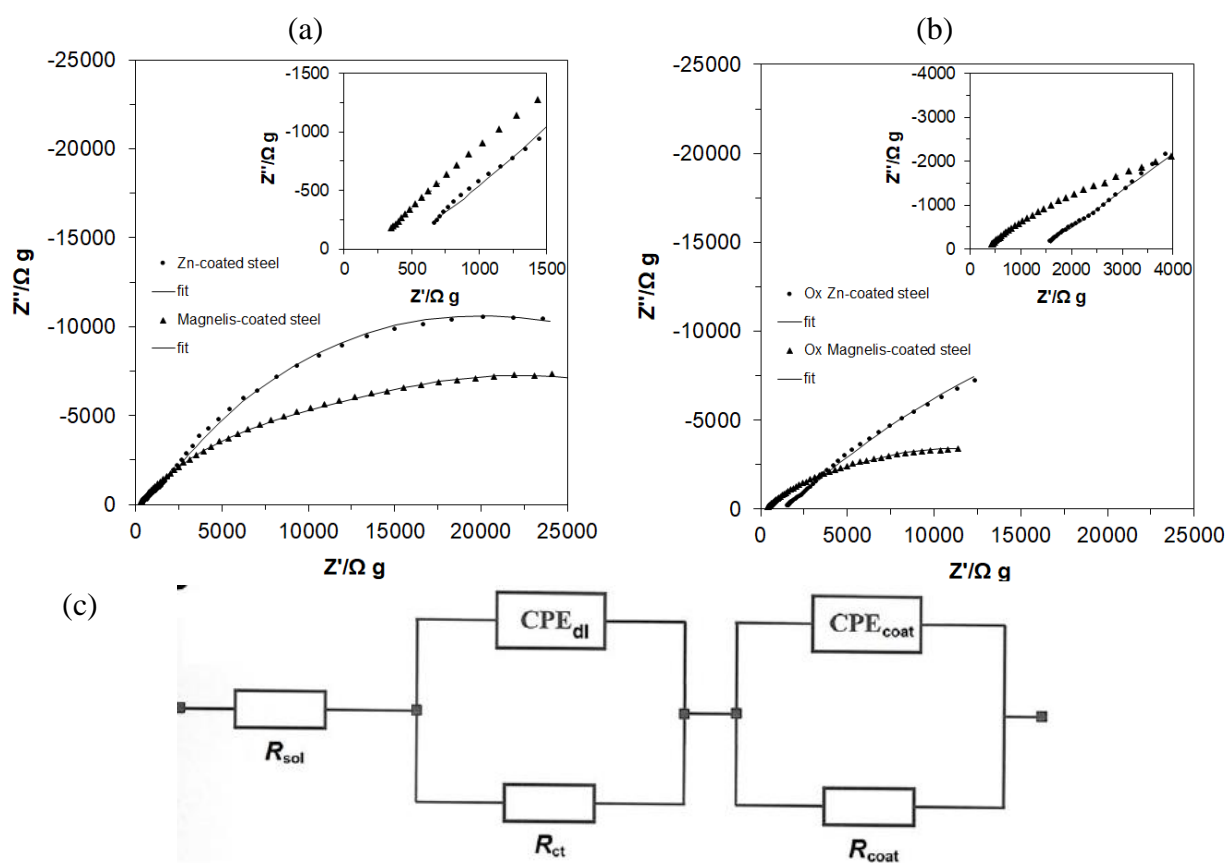
Figure 3. The impedance plots for: (a) Magnelis®-coated and hot-dip Zn-coated steel electrodes, registered at corresponding corrosion potentials at room temperature in self-aerated 0.1 M Na_2SO_4 solution and pH 7 and (b) Magnelis®-coated and hot-dip Zn-coated steel electrodes, recorded in O$_2$-saturated 0.1 M Na_2SO_4 solution and pH 7; (c) Two CPE-R element equivalent circuit model used for fitting the impedance data. The circuit consists of double constant phase elements (CPEs) to balance the effect of distributed capacitance; CPE$_{coat}$ and R_{coat} elements are related to the capacitance of surface and resistance corrosion products; CPE$_{dl}$ and R_{ct} correspond to the interfacial double-layer capacitance and reaction charge-transfer resistance parameters, and R_{sol} is the resistance of the solution.

4. CONCLUSIONS

In this study, the authors comparatively provided information on initial corrosion behaviour of typical hot-dip Zn-coated steel and innovative Magnelis®-coated steel materials, examined in the function of changing environmental conditions (0.1 and 0.5 M Na_2SO_4 solution, pH range: 3-11 and under two electrolyte aeration states). The following conclusions have been drawn:

1. Initial, short-term exposure of Zn(Magnelis®)-coated samples proved that Magneli® material remains significantly more resistant to a wide range and various corrosion atmospheric conditions (including salt concentration, electrolyte pH and oxygen content) as compared to a typical industrially-made hot-dip Zn coated material;

2. Exclusive corrosion behaviour of Magnelis® material is related to the fact that its Al and Mg elemental modifiers (under working conditions) provide the additional surface formation of the complex (Mg/Al) hydroxy carbonate precipitates, thus delivering superior protection to the base material and partial inhibition of the cathodic oxygen depolarization reaction;

3. Additional laboratory work is needed in order to provide details on the respective, long-time corrosion behaviour of these two technologically competing materials, under the examined range of environmental parameters.

References

1. A. Mardani, A. Jusoh, E. K. Zavadskas, F. Cavalarro, Z. Khalifah, *Sustainability*, 7 (2015) 13947.
2. N. L. Panwar, S. C. Kaushik, S. Kothari, *Renew. Sust. Energ. Rev.*, 15 (2011) 1513.
3. M. R. S. Shaikh, S. B. Waghmare, S. S. Labade, P. V. Fuke, A. Tekale, *Int. J. Res. Appl. Sci. Eng. Technol.*, 5 (2017) 1184.
4. M. Babula, *J. Edc. Health Sport*, 7 (2017) 136.
5. H. Liu, V. Krishna, J. L. Leung, T. Reindl, L. Zhao, *Prog. Photovolt. Res. Appl.*, 26 (2018) 957.
6. Z. A. Kamargyzzaman, A. Mohamed, H. Shareef, *Prz. Elektrotechniczn.*, 1 (2015) 136.
7. O. I. Sekunowo, S. O. Adeosun, O. E. Ojo, *Int. J. Eng. Technol.*, 4 (2014) 325.
8. M. Vaghani, S. A. Vasanwala, A. K. Desai, *Int. J. Eng. Res. Appl.*, 4 (2014) 657.
9. E. C. Chinwko, B. O. Odio, J. L. Chukwuneke, J. E. Sinebe, *Int. J. Sci. Technol. Res.*, 3 (2014) 306.
10. L. Klimek, J. Waś-Solipiwo, K. Dybowski, *Adv. Sci. Technol. Res. J.*, 11 (2017) 28.
11. Y. Li, *B. Mat. Sci.*, 24 (2001) 355.
12. M. Mouanga, M. Puiggali, B. Tribollet, V. Vivier, N. Pébère, O. Devos, *Electrochim. Acta*, 88 (2013) 6.
13. Z. Samsu, M. Daud, S. R. M. Kamarudin, N. U. Saidin, A. A. Mohamed, M. S. Ripin, R. Rejab, M. S. Sattar, *J. Nucl. Rel. Technol.,* 8 (2011) 78.
14. H. A. Al-Mazeedi, A. Al-Farhan, N. Tanoli, L. Abraham, *Int. J. Corros.*, 2019 (2019) 1.
15. S. J. Suess, *J. Systemics Cybernetics Inform.*, 4 (2006) 73.

16. T. Alemayehu, M. Birahane, *Int. J. Acad. Sci. Res.*, 2 (2014) 1.
17. H. Kajiama, S. Fujita, M. Sagiyama, *JFE Tech. Rep.*, 9 (2007) 80.
18. K. Hayashi, Y. Ito, Y. Miyoshi, *Nippon Steel Tech. Rep.*, 63 (1994) 8.
19. O. S. I. Fayomi, A. P. I. Popoola, *Int. J. Electrochem. Sci.*, 7 (2012) 6555.
20. https://industry.arcelormittal.com/flipflop/fce/Brochures/Magnelis_book_EN/index.html, accessed in June, 2019.
21. B. Pierozynski, H. Bialy, *Electrocatalysis*, 9 (2018) 416.
22. B. A. Mei, O. Munteshari, J. Lau, B. Dunn, L. Pilon, *J. Phys. Chem. C*, 122 (2018) 194.
23. Y. Hamlaoui, F. Pedraza, L. Tifouti, *Am. J. Appl. Sci.*, 4 (2007) 430.
24. Y. Liu, H. Li, Z. Li, *Int. J. Electrochem. Sci.*, 8 (2013) 7753.
25. H. Sun, S. Liu, L. Sun, *Int. J. Electrochem. Sci.*, 8 (2013) 3494.
26. S. Liu, H. Sun, N. Zhang, L. Sun, *Int. J. Corros.*, 2013 (2013) 1.
27. Y. Hamlaoui, F. Pedraza, L. Tifouti, *Corros. Sci.*, 50 (2008) 1558.
28. B.E. Conway, Impedance Spectroscopy. Theory, Experiment, and Applications, John Wiley, (2005) Hoboken, USA.
29. W. G. Pell, A. Zolfaghari, B. E. Conway, *J. Electroanal. Chem.*, 13 (2002) 532.
30. S. Liu, H. Sun, N. Zhang, L. Sun, *Int. J. Corros.*, 2013 (2013) 1.
31. M. Salgueiro Azevedo, C. Alley, K. Ogle, P. Volovitch, *Corros. Sci.*, 90 (2015) 472.
32. N. C. Hosking, M. A. Ström, P. H. Shipway, C. D. Rudd, *Corros. Sci.*, 49 (2007) 3669.
33. J. Rodriguez, L. Chenoy, A. Roobroeck, S. Godet, M. G. Olivier, *Corros. Sci.*, 108 (2016) 47.
34. E. Hakansson, J. Hoffman, P. Predecki, M. Kumosa, *Corros. Sci.*, 114 (2017) 10.
35. M. Dutta, A. K. Halder, S. B. Singh, *Surf. Coat. Technol.*, 205 (2010) 2578.
36. M. Salgueiro Azevedo, C. Allély, K. Ogle, P. Volovitch, *Corros. Sci.*, 2014 (2014) 1.
37. E. Diler, B. Rouvellou, S. Rioual, B. Lescop, G. Nguyen Vien, D. Thierry, *Corros. Sci.*, 87 (2014) 111.
38. B. Pierozynski, H. Bialy, *Pol. J. Chem. Technol.*, 19 (2017) 22.